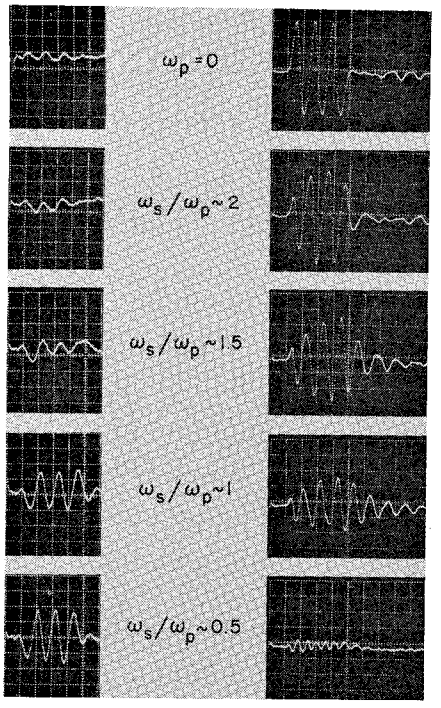

Fig. 2. Observed dispersion of sinusoidal pulses in a plasma-filled coaxial line. Time scale 2 ns per division, pulse duration 3 cycles. (a) pulse reflected from plasma-air interface. (b) pulse transmitted through plasma ($d=1.5$ m, $\theta\sim15$).

necting transmission line. The reflection of the wavetrain at the interface between the coaxial line and the connecting cable is shown in Fig. 2(a) ($\omega_p=0$). The RF pulse proceeds essentially undistorted through the coaxial line, where it is detected by a small field probe [Fig. 2(b) ($\omega_p=0$)]. A spurious response, delayed by approximately 12 ns, is caused by rereflection of the main pulse after its repassing twice through the coaxial line. The enhanced reflection of the pulse and the distortion of the transmitted pulse caused by the plasma are shown in the following exposures [Figs. 2(a) and 2(b)], observed at various times in the afterglow corresponding to different values of the plasma frequency. In an underdense plasma ($\omega_s/\omega_p=2$ and 1.5), the reflection remains small. The reflected signal, and particularly the transmitted signal, show the development of a pronounced transient ringing near the plasma frequency. The duration of the observed transient is longest for a plasma with near-critical electron density ($\omega_s/\omega_p\sim1$). Clearly, the received signal bears little resemblance to the original short-pulse train. In an overdense plasma ($\omega_s/\omega_p\sim0.5$), the reflection is large as the main pulse is cut off in the plasma. The small transmission observed arises from frequency components of the pulse spectrum near and beyond the plasma frequency, enhanced by spurious components near the harmonic of the carrier frequency due to imperfect sinusoidal-pulse shape. In a thin plasma layer, a weak tunneling of the attenuated main pulse is also observed [4]. For a comparison with the calculated results, note that for the transmitted signal, interface reflections which tend to reduce the transient duration have been neglected in the theoretical response.

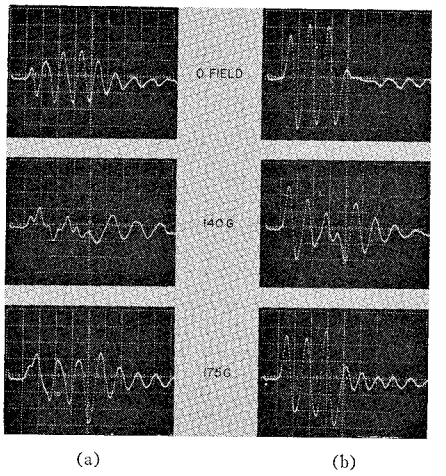

Fig. 3. Dispersion of a sinusoidal pulse in a longitudinally-magnetized plasma in a coaxial line. Time scale 2 ns per division, magnetic field in gauss. (a) $\omega_s/\omega_p\sim1$. (b) $\omega_s/\omega_p\gg1$.

The complexity of the dispersion process is increased if static magnetic fields are superimposed on the plasma. For a longitudinally magnetized plasma in a coaxial line, one obtains a dispersion relation [5]

$$k^2=\frac{\omega^2}{c_0^2}\left(1-\frac{\omega_p^2}{\omega^2-\omega_c^2}\right) \qquad (5)$$

which reflects pass bands below the angular electron-cyclotron frequency ω_c and above the hybrid frequency $\omega_h=\sqrt{\omega_p^2+\omega_c^2}$. The distortion of a wave pulse will depend on the relation between its carrier frequency and the natural frequency of the plasma.

We have observed experimentally the gross effects on the pulse dispersion introduced by a magnetic field set up by a long solenoid surrounding the plasma-filled coaxial line. The results, as shown in Fig. 3(a), indicate that for a plasma with near-critical electron density, a weak magnetic field tends to suppress the main pulse (Fig. 3(a), 140 gauss) as the upper cutoff frequency is shifted from ω_p to ω_h. The pulse is distorted into a weakly damped ringing, approaching in time the cyclotron frequency and arising from frequency components in the lower pass band $\omega<\omega_c$. With further increasing magnetic field, the main pulse is again observed when the lower pass band extends to frequencies $\omega_c>\omega_s$. The distortion vanishes for $\omega_c\gg\omega_s$, where transverse motion of electrons is inhibited by the strong magnetic field. The characteristic ringing at the electron-cyclotron frequency is particularly well observed in a tenuous plasma (Fig. 3(b)) where negligible distortion of the transmitted pulse occurs in the absence of magnetic fields. A nearly undamped oscillation at the cyclotron frequency trails the direct signal (Fig. 3(b), 175 gauss). Similar transient oscillations are also observed in the reflected pulse shape.

Acknowledgment

The author wishes to thank J. Morris for help extended in the experiment.

H. J. Schmitt
Sperry Rand Research Ctr.
Sudbury, Mass.

References

[1] Schmitt, H. J., Plasma diagnostics with short electromagnetic pulses, *IEEE Trans. on Nuclear Science*, vol NS-11, Jan 1964, pp 125–136.
[2] Schmitt, H. J., Pulse dispersion in a gyrotropic plasma, to be published.
[3] Knop, C. M., Pulsed electromagnetic wave propagation in dispersive media, *IEEE Trans. on Antennas and Propagation*, vol AP-12, Jul 1964, pp 494–496.
[4] Case, C. T., Transient reflection and transmission of a plane wave normally incident upon a semi-infinite anisotropic plasma, Phys. Sci. Research Papers 33, 64-550, Microwave Physics Lab., 1964.
[5] Mower, L., Propagation of bounded electromagnetic waves within an anisotropic plasma, Tech Rept 4, Sylvania Microwave Physics Lab., Mountain View, Calif., 1957.

Injection Locking of a Laddertron at 35 Gc/s

An OKI 34LV10 Laddertron was locked at 34 830 Mc/s by injecting a controlling signal into the Laddertron cavity. The Laddertron is a single-cavity multigap oscillator that can deliver about 10 watts CW. The controlling signal was obtained from a klystron that was phase locked to a crystal oscillator harmonic. The Laddertron can be locked for CW or for pulse operation.

Phase locking of microwave oscillators is usually accomplished by using an intermediate frequency offset. The principal advantage of this method is that the reference power required is only what is needed to operate a limiter in the IF amplifier. The disadvantages are a) electronic circuits are required, b) a microwave directional coupler and mixer are required, and c) the spectrum of the output is that of the reference input only within the pass band of the lock loop (typically 100 kc) so that the electronic loop determines the modulation capability. Therefore, frequency control is not possible for pulse operation.

The injection-locked system requires no electronic circuitry and the modulation capability is determined by the response time of the locked oscillator. The only microwave component needed is a circulator. The main disadvantage is that more reference power is required; the reference power for the IF phase lock can be obtained from a maser oscillator (10^{-10} watts) or from a harmonic of a crystal driven by an RF source while the reference power for the injection lock is typically 30 dB below the oscillator output.

Adler's theory [1] of oscillator synchronization was verified for X-band reflex klystrons by Mackey [2]. The locking relationship is

$$\left[\frac{2Q\Delta f}{f_0}\left(\frac{P_0}{P_1}\right)^{1/2}\right]=\sin\phi \qquad (1)$$

where

P_0 = oscillator output power
P_1 = injected input power
$\Delta f=f_0-f_1$
f_0 = free-running oscillator frequency
f_1 = injected input frequency

Manuscript received March 18, 1965.

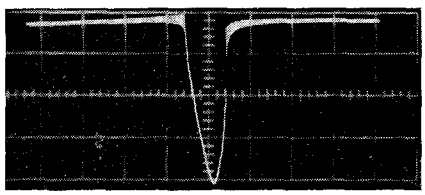

Fig. 1. Locking range of Laddertron, power injected =17 mV, power output=5 W, center frequency 34 830 Mc/s, frequency sweep=5 Mc/div, oscillator Q=408, [calculated from (1)].

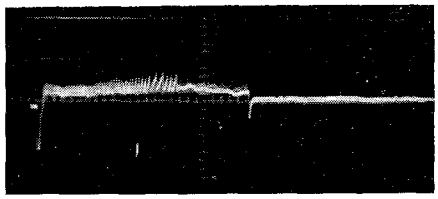

Fig. 2. Laddertron locking in pulsed mode, locked frequency=34 830 Mc/s, sweep speed=2×10^{-5} s/div, pulse width=10^{-4} s, pulse power=5 W, injected power 1mW.

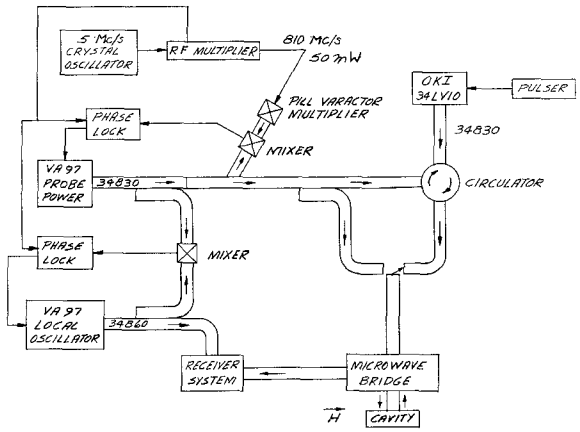

Fig. 3. Simplified block diagram of EPR spectrometer.

Q=figure of merit of the loaded oscillator cavity

ϕ=phase difference between the injected input signal and the locked output.

The locking range of the Laddertron is illustrated by Fig. 1 which shows the output of a crystal detector monitoring the reference input. Enough Laddertron output is also coupled so the mixed output is observed. The reference input is swept 40 Mc/s at 34 830 Mc/s. The video beat between the input and output is observed just before and just after locking. The lock range is 5 Mc/s. Since the response time of the oscillator is much faster than the sweep, (1) can be used to compute the loaded oscillator Q by noting the end points of the lock range which correspond to $\phi=\pm90^0$. The dc level gives a convenient indication of the midpoint of the lock range.

Figure 2 is an oscilloscope trace of the mixed output when the reference signal was phase locked to a harmonic of a crystal oscillator and the Laddertron was pulsed on with 100-μs pulses. The injection power was reduced about 20 dB to observe the time required for locking. In the figure the Laddertron locks about 70 μs after the start of the pulse. As the reference power was increased to 17 mW, the time required for locking decreased to less than 1 μs. The synchronization time could not be accurately measured by this method.

Figure 3 is a block diagram of an electron paramagnetic resonance spectrometer. The Laddertron is used for pulse-relaxation time measurements and for the high-power multiple-quantum effects. All three tubes are locked to harmonics of the 5 Mc/s frequency standard. The probe power tube has to be phase locked by the IF offset method because the reference power from the pill varactor is low. The local oscillator is locked to the probe power by a 30-Mc/s IF phase lock. With a superheterodyne system the magnetic modulation frequency can be low (39 c/s) and by using phase-locked klystrons the IF bandwidth can be made as narrow as possible by using a crystal filter. The probe power is used to injection lock the Laddertron. The Laddertron could be locked for CW operation by the IF method but the modulation sensitivity is so low (0.2 Mc/s/V) that very high IF voltages or dc amplification of the correction signal would be required for satisfactory operation. For pulse work the injection method is required.

Improved frequency multipliers will allow the Laddertron to be locked to a crystal harmonic without the intermediate klystron.

R. G. Strauch
W. T. Smith
V. E. Derr
The Martin Co.
Orlando, Fla.

References

[1] Adler, R., A study of locking phenomena in oscillators, *Proc. IRE*, vol 34, Jun 1946, pp 351–357.
[2] Mackey, R., Injection locking of klystron oscillators, *IRE Trans. on Microwave Theory and Techniques*, vol MTT-10, Jul 1962, pp 228–235.

Nonreciprocal Directional Couplers

This correspondence is concerned with 1) the modifications required in the standard scattering-matrix description of a directional coupler [1] when the constraint of reciprocity is dropped, and 2) the advantages of using a nonreciprocal directional coupler (NRDC) in place of a conventional reciprocal directional coupler (DC) in a traveling-wave resonant circuit.

A survey of the literature reveals that those investigators who specifically studied the NRDC, such as Damon [2], Berk and Strumwasser [3], and Stinson [4], were concerned with the physics of specific models, and did not discuss the four-port characteristics of the general NRDC. On the other hand, those investigators who dealt with the more general descriptions of nonreciprocal four-ports, such as Fox [5] and Davison [6], were primarily interested in determining conditions under which a cascade of various structures would act as a circulator. More recently, Skeie [7] discussed nonreciprocal coupling of a specific type, and some characteristics of nonreciprocal four-ports but did not explore the NRDC.

To the author's knowledge the scattering matrix representation, presented below and derived elsewhere [8], of a general NRDC, (i.e., a lossless nonreciprocal matched four port with two distinct pairs of uncoupled ports) is not available in the general literature.

The standard condition for losslessness is that the scattering matrix $S=(S_{ij})$ is unitary, i.e., $S^+S=1_4$ where $(S_{ij})^+\equiv(S_{ji}{}^*)$ is the complex conjugate of the transpose of S, and 1_4 is the unit four-by-four matrix. For a matched four-port, we require $S_{ii}=0$ $(i=1, 2, 3, 4)$, and for the decoupled ports we have $S_{13}=S_{31}=S_{24}=S_{42}=0$. These constraints are satisfied if

$$S=\begin{pmatrix} 0 & \sqrt{1-C_1^2}\,e^{j\theta_{12}} & 0 & C_1e^{j\theta_{14}} \\ \sqrt{1-C_2^2}\,e^{j\theta_{21}} & 0 & C_2e^{j\theta_{23}} & 0 \\ 0 & C_1e^{j\theta_{32}} & 0 & \sqrt{1-C_1^2}\,e^{j\theta_{34}} \\ C_2e^{j\theta_{41}} & 0 & \sqrt{1-C_2^2}\,e^{j\theta_{43}} & 0 \end{pmatrix} \tag{1}$$

where

$$(\theta_{32}-\theta_{12})+(\theta_{14}-\theta_{34})=\pi \tag{2}$$

$$(\theta_{41}-\theta_{21})+(\theta_{23}-\theta_{43})=\pi \tag{3}$$

and where we shall refer to C_1 as the forward-coupling coefficient, and to C_2 as the backward-coupling coefficient.

For a conventional DC, the phase difference between the output waves produced by an input to any one of the four-ports [represented by the bracketed terms in (2) and (3)] are separately equal to $\pi/2$. From (2) and (3) we observe that for a NRDC, the sum of such phase differences in output waves generated by an input applied to any one port, and separately to the port isolated from that first port, are π. If (2) is sub-

Manuscript received March 26, 1965. The work reported herein was sponsored in part by the Rome Air Development Center, under Contract AF-30(602)-2135.